Inelastic Gravitational Billiards

S. Feldt and J. S. Olafsen*

Department of Physics and Astronomy, University of Kansas, Lawrence, Kansas 66045, USA

(Received 23 November 2004; published 7 June 2005)

We present an experimental investigation of gravitational billiards where the particle undergoes inelastic collisions with its boundary. The motion is mapped for an inelastic particle contained within parabolic, wedge, and hyperbolic boundaries. For the parabola, stable orbits are found and the wedge demonstrates a characteristic instability for its vertex angle. In the instance of the hyperbola, there are several features of the dynamics similar to the parabola at low driving and the wedge for higher driving. However, the low driving case for a hyperbola can only be completely understood by considering inelasticity effects predicted by a numerical simulation and the observation that the velocity dependent inelasticity allows the particle to sample several nearby trajectories for fixed driving.

DOI: 10.1103/PhysRevLett.94.224102 PACS numbers: 05.45.Ac, 02.30.Ik, 45.20.Jj

Gravitational billiards are a rich system for studying instability and chaos in Hamiltonian dynamics where the shape of the boundary governs the observed motion of the particle [1–3]. Not surprisingly, parabolic boundaries demonstrate stable orbits whose amplitude is determined by the energy of the billiard [1], while the wedge boundary demonstrates both unstable and chaotic behavior dependent upon the value of the vertex angle of the wedge [2]. An even more interesting case is that of a hyperbolic boundary that demonstrates parabolic behavior for orbits near its origin and wedge behavior for orbits near its asymptotes [3]. The motion of a particle in a wedge has been experimentally demonstrated for an optical billiard with ultra cold particles [4]. Here, we present a new experimental realization for two-dimensional parabolic, wedge, and hyperbolic geometries where the particle undergoes inelastic collisions with the confining boundaries in the presence of a gravitational potential. Inelastic collisions have been shown to lead to clustering [5] and inelastic collapse [6]. A prior investigation analytically and numerically investigated the behavior of a particle of variable elasticity within an effective wedge boundary to search for effects of clustering and inelastic collapse [7]. In this experiment, evidence is obtained of stable, unstable, period doubling, and chaotic dynamics for the billiard contained within the different boundaries. While the energy injection to the system is maintained at a fixed value, the inelasticity allows the particle to move between nearby trajectories, demonstrating a variety of orbits at fixed energy input.

The experiment consists of a steel frame with an interior square of 16.5 cm $\times$ 16.5 cm into which a 3.2 mm thick wedge, parabolic, or hyperbolic aluminum insert can be placed vertically with respect to gravity to examine the motion of a 3.1 mm diameter chrome steel ball within the selected boundary. The coefficient of restitution between the ball and the aluminum boundary is approximately 0.9 but is known to be velocity dependent [8]. Sheets of Plexiglas constrain the motion of the particle to a thin 2D layer and at the same time allow for observation of the particle's motion. The vertical cell is seated on a linear bearing that constrains the motion of the cell to a horizontal line along the plane of the boundary. A wheel and linking armature converts the rotational motion of the Dayton 1/8 hp dc motor into a sinusoidal horizontal motion of the cell on the linear slide. The frequency of oscillation, ν, was varied between 4–7 Hz, and the peak-to-peak amplitude of oscillation was held constant at $A = 2.54$ cm for the results presented in this paper.

The system is started from rest and the particle's motion is soon ballistic across the cell. The energy lost in the collisions is compensated by the horizontal driving of the cell whose peak acceleration is given by $\Gamma = A\omega^2$ where $\omega = (2\pi\nu)^2$. Thus by increasing and decreasing ν, the total energy of the system is increased or decreased. For imaging purposes, a second identical chrome steel particle is imbedded in each of the boundary inserts beneath the vertex of each surface, so that high-speed CCD imaging could track both the motion of the cell and the particle moving ballistically within the cell [9]. Programs written in IDL [10] are used to track the particle's trajectory and extract the particle's velocity before and after these collisions. A mapping is then made to relate the velocity and position of one collision point to the velocity and position at the following collision point.

Figure 1(a) shows the shape of these boundaries and their orientation with respect to gravity and the external driving. The boundaries are offset for clarity. Figs. 1(b)–1(d) each show a picture of the particle in motion as imaged for the parabolic, wedge, and hyperbolic boundaries, respectively. In order to compare the experimental results to the previous numerical investigation of a hyperbolic geometry for an elastic particle [3], the particular parabola and wedge surfaces were chosen to approximate the hyperbola in different regimes. Near their centers, the hyperbola and the parabola are nearly congruent and, near its extent, the hyperbola asymptotes to the particular wedge chosen.

The parabolic boundary is given by $y = ax^2 + c$, the wedge is given by $y = b|x| + c$, and the hyperbolic boundary by $y = \sqrt{\alpha(1 + \beta x^2)} - \delta$. For these experi-

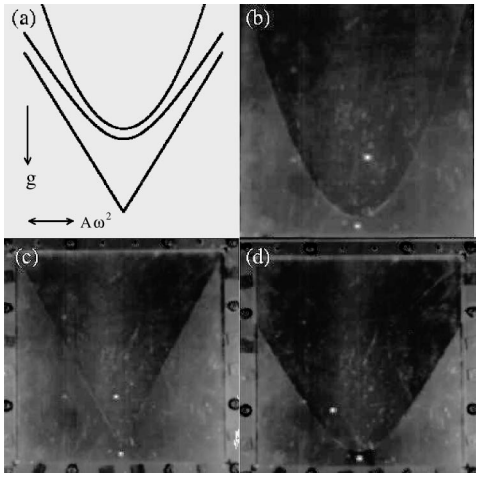

FIG. 1. (a) A schematic of the boundaries used in the experiment. An image of the particle in motion in the parabolic (b), wedge (c), and hyperbolic (d) boundaries.

ments, $a = 0.26\ \mathrm{cm}^{-1}$, $b = 1.85$, $c = 0.63$ cm, $\alpha = 40.3\ \mathrm{cm}^2$, $\beta = 0.08\ \mathrm{cm}^{-2}$, and $\delta = 4.45$ cm for x and y both in centimeters.

In order to completely describe the phase space of the 2D system four parameters would be required. However, to easily view the dynamics of the system, this four-dimensional phase space is projected onto a two-dimensional area. Traditionally, Birkhoff coordinates are the natural choice for examining billiards [11], allowing closed orbits to be described with p reflections in q cycles around the boundary. However, for the case of gravitational billiards, where the free particle is acted upon by gravity between collisions, it is helpful to examine the system with more carefully chosen coordinates to map the orbits [2].

The energy of the particle at a collision point is given by $E = mv^2/2 + mgy$ where v is the velocity of the particle immediately after a collision, m is the mass of the particle, g is the acceleration due to gravity, and y is the height of the particle at the collision point. We can then use this energy to calculate a maximum possible value for the height of the collision $y^{\max}$, if all of the energy were potential energy, and a maximum possible tangential component of the velocity $v_t^{\max}$, for the particle if all of the energy were kinetic:

$$y^{\max} = \frac{E}{mg} = \frac{v^2}{2g} + y \tag{1}$$

$$v_t^{\max} = \sqrt{\frac{2E}{m}} = \sqrt{v^2 + 2gy}. \tag{2}$$

Note that this phase space projection must lie under the envelope given by plotting $y/y^{\max}$ as a function of $v/v^{\max}$, where v is the total velocity of the particle after the collision. It is helpful to decompose the velocity into normal and tangential components relative to the local surface where the collision occurs. A completely stable period-one orbit for a symmetric boundary would have a zero tangential velocity component, each collision occurring normal to the local surface.

Figure 2 shows sample trajectories of the particle's motion within a particular boundary. The trajectories shown here depict the motion of the free particle relative to the motion of the cell. Those portions of the trajectories where the slope of the ballistic motion changes while the free particle is in flight correspond to moments where the velocity of the cell changes direction.

Figure 2(a) demonstrates the characteristic stable motion of the particle within the parabola driven at 5.4 Hz. As the driving frequency (and therefore energy) is increased or decreased, the average orbit moves up or down, respectively, within the parabola. The inelasticity and surface roughness allow the particle to move from one nearby stable orbit to another over long periods of time at fixed driving.

Figure 2(b) shows a sample trajectory of the particle within the wedge when driven at a frequency of 6.6 Hz. The motion of an elastic billiard within a wedge is dependent upon the half vertex angle of the wedge. For half angles below 45 degrees, coexisting stable and unstable motion can occur [2,4]. For our half angle of 28.5 degrees, we observe this unstable motion as the inelastic particle is repeatedly driven toward the top of the boundary.

In Fig. 2(c), we present a sample trajectory of the particle contained within the hyperbolic boundary when driven at a frequency of 4.5 Hz. Interestingly, the particle's motion is not stable, and the particle explores the phase space over longer periods of time. Figure 2(d) shows a trajectory of the particle within the hyperbola when the frequency has been increased to 5.8 Hz. The times of flight

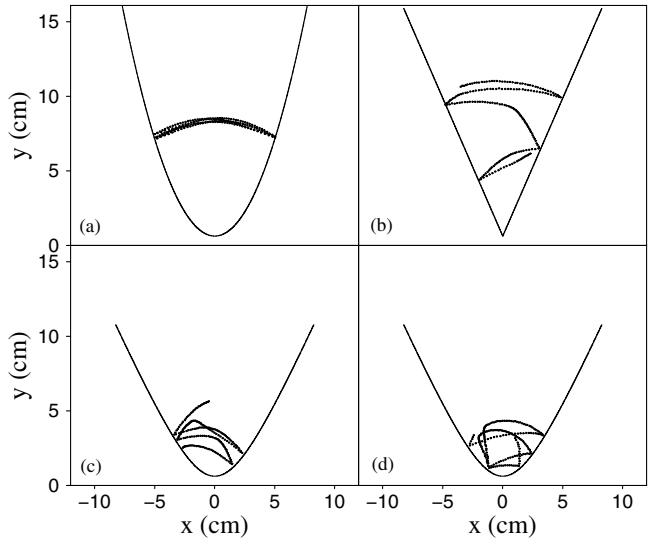

FIG. 2. Sample trajectories of the particle with respect to the motion of the cell for (a) the parabola driven at a frequency of 5.4 Hz, (b) the wedge at 6.6 Hz, (c) the hyperbola at 4.5 Hz, and (d) the hyperbola at 5.8 Hz.

between collisions are approximately 0.041 and 0.122 s for a half driving period of 0.086 s, indicative of a period-two orbit over brief time periods. However, the noise present in the system, combined with the inelasticity of the particle, causes the particle to quickly transition to unstable behavior and to be driven to the top of the hyperbola, similar to the case of the wedge.

To examine the behavior over longer periods of time, the height at one collision is plotted versus the height at the following collision, producing a map of the motion in the left column of Fig. 3. The dashed lines in the figure are the $y_n = y_{n+1}$ return map that would denote stable period-one orbits. The right column of Fig. 3 shows the time of flight between collisions versus the time of flight from the next collision. Figure 3(a) shows the y positions for the case of the parabola driven at 5.4 Hz. The quasistable orbit of the parabola is easily seen as the collisions map to nearly the same spot in both the positional and temporal maps. The inelastic nature of the collisions slightly alters the velocity of the particle, and because the coefficient of restitution is velocity dependent, this feeds back into the long time behavior of the particle. The trajectory of the particle is not simply a single stable orbit, but rather accesses several nearby stable orbits, resulting in an elongation of the stable fixed point along the direction of the slope 1 line. Similarly, this leads to a slight smearing of the collision times as can be seen in Fig. 3(b).

Figure 3(c) shows the map of y positions of the particle collisions within the wedge driven at 6.6 Hz. The motion is clearly unstable and the particle is continuously driven to the top of the wedge. The data below the return map is indicative of how the particle behaves after striking the top of the cell enclosure. In Fig. 3(d), the unstable behavior is represented in terms of the collision times as well as an apparent period-two behavior, a coexisting stable dynamic that one would expect for the selected vertex angle.

In Fig. 3(e) we examine the y positions of the particle collisions within the hyperbolic boundary when driven at 4.5 Hz. The motion here is very different from the other cases and appears to attempt to fill the space, not simply mimicking behavior for the approximately parabolic surface of the hyperbola at low energy. Examining the times of flight in Fig. 3(f), we notice that the behavior here is unusual as well and there appears to be a sort of banding in the data, unlike Fig. 3(b). This banding is representative of a fractal behavior as seen by Grossman and Mungan when studying inelastic billiards [7]. They found that this fractal behavior occurred in the slightly inelastic regime, which one would expect in this experiment for low driving. We know that the coefficient of restitution of our particle is velocity dependent. Therefore, as the driving frequency is increased, the coefficient of restitution will drop and the particle will become increasingly inelastic. This explains why we only observe this special behavior for low driving frequencies. In addition, the simulations by Grossman and Mungan suggest that the formation of the fractal behavior is robust and should correspond to a globally attractive region of phase space. As we will show in Fig. 4, the fractal behavior coincides with a global stable point in phase

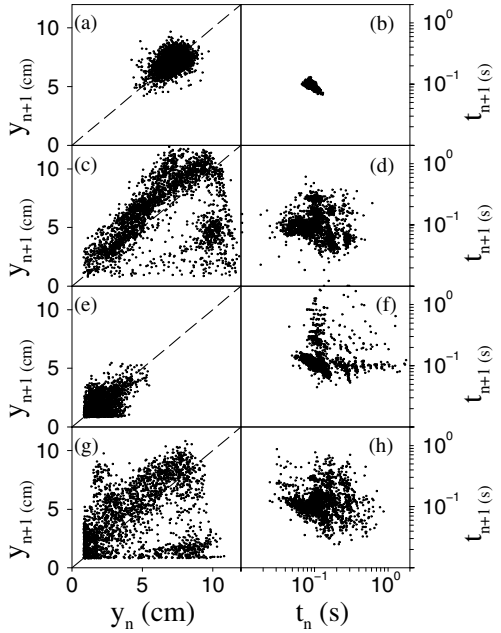

FIG. 3. The mappings of the collision heights (left column) and the times of flight (right column). In (a) and (b) we see the parabola at 5.4 Hz, (c) and (d) show the wedge at 6.6 Hz, (e) and (f) show the hyperbola at 4.5 Hz, and (g) and (h) show the hyperbola at 5.8 Hz.

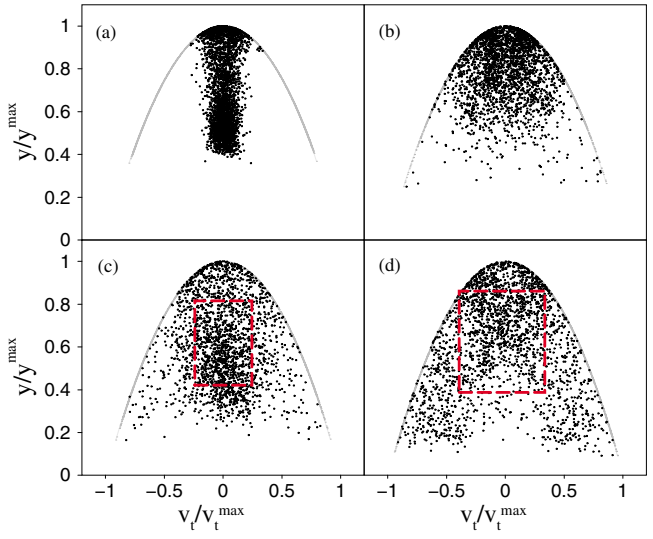

FIG. 4 (color online). Plots of $y/y^{\max}$ as a function of $v_t/v_t^{\max}$, where v_t is the tangential component of the velocity, for the case of (a) the parabola driven at 5.4 Hz, (b) the wedge driven at 6.6 Hz, (c) the hyperbola driven at 4.5 Hz, and (d) the hyperbola driven at 5.8 Hz. The data falls within the envelope (gray line) given by $y/y^{\max}$ as a function of $v/v^{\max}$, where v is the total velocity.

space that disappears along with the fractal behavior at higher driving.

When the driving frequency is increased to 5.8 Hz as in Figs. 3(g) and 3(h), as expected, we no longer see this fractal behavior and the motion is unstable resembling the case of the wedge. In the time of flights depicted in Fig. 3(h), we again see temporal behavior similar to the case of the unstable wedge.

In Fig. 4(a) we show $y/y^{\max}$ versus $v_t^{\max}$ for the parabola driven at 5.4 Hz. The tangential component of the velocity is in a thin band about zero, indicating a stable orbit. While an attractor can be clearly seen in the center of the phase space, the $y/y^{\max}$ values explore much of the phase space in this thin window of tangential velocity. This is due to a combination of the noise in the system and the inelasticity of the particle. Since the x position is uniquely determined by the height of the collision, and the tangential velocity is tightly confined about zero, the variations in the $y/y^{\max}$ values are directly related to the variations in the normal velocity component. Even the small variations present in the velocity of the particle (chiefly in the normal component) will change the coefficient of restitution of the particle, causing a spread in the $y/y^{\max}$ values as the particle collides with the boundary over several oscillations.

For the case of the wedge at 6.6 Hz in Fig. 4(b), the particle explores a range of velocities, in both tangential and normal components, and the stable attractor in the middle of the phase space plot is no longer present. The particle spends most of its time near the top of the envelope near its maximum y value. This is consistent with the wedge's ability to continuously drive the particle upwards.

When the particle is confined within the hyperbolic boundary, it explores more of the phase space in general as seen in Figs. 4(c) and 4(d). Figure 4(c) shows the hyperbola driven at 4.5 Hz. At this lower energy, the particle explores a range of y and v_t values; however, in the middle of the space, there is again evidence of an attractor similar to that of the parabolic case, yet the tangential component of the velocity is not as narrowly constrained. In Fig. 4(d) the driving frequency has been increased to 5.8 Hz, clearly eliminating any attractor that was present in the case of the low driving frequency. In fact, the particle shows a predominant tendency to explore its maximum y and v_t values as in the case of the wedge, with a decreased frequency of period-two behavior [Fig. 3(h)]. The dashed boxes in Figs. 4(c) and 4(d) denote a region of phase space within 1 standard deviation of the mean for each variable. It is interesting to observe that the fractal-like behavior occurs for the lower driving when the system has less phase space to explore. This is also in agreement with the simulation of an elastic particle within a hyperbolic boundary [3] that found chaotic behavior at lower energies and regions of decreased phase space. However, if the dissipation of the inelastic collisions were simply another form of noise, one would expect Figs. 3(b), 3(f), 4(a), and 4(c) to be identical, with perhaps some broadening. Instead, what is observed in the case of low driving in the hyperbola is an additional effect of inelasticity in the banding of the times of flight in the presence of a stable attractor in agreement with Grossman and Mungan [7].

We have presented a new experimental method for exploring two-dimensional gravitational billiards. Using a horizonal driving force to maintain the dynamics, we were able to observe results similar to the numerical studies that have been done with elastic particles scattered within parabolic, wedge, and hyperbolic boundaries. In the case of the parabola, the motion was that of a stable orbit, while it was unstable in the case of the wedge. At low driving frequencies (energies), the motion of the particle within the hyperbola showed fractal behavior in collision times and a filling of the phase space indicative of chaos. At higher driving frequencies, the motion of the particle within the hyperbola resembled that of the unstable motion within a wedge. This method of exploring experimental gravitational billiards proves promising for future studies of the dynamics of motion for gravitational billiards in the case where the particle is inelastic and invites further theoretical analysis.

This research was supported by a grant from Kansas NASA EPSCoR and grants from both the UGRA and GRF programs at the University of Kansas.

*Electronic address: jolafsen@ku.edu

[1] H. Korsch and J. Lang, J. Phys. A **24**, 45 (1991).
[2] H. Lehtihet and B. Miller, Physica (Amsterdam) **21D**, 93 (1986).
[3] M. Ferguson, B. Miller, and M. Thompson, Chaos **9**, 841 (1999).
[4] V. Milner, J. Hansen, W. Campbell, and M. Raizen, Phys. Rev. Lett. **86**, 1514 (2001).
[5] I. Goldhirsch and G. Zanetti, Phys. Rev. Lett. **70**, 1619 (1993).
[6] S. McNamara and W. R. Young, Phys. Rev. E **53**, 5089 (1996).
[7] E. Grossman and M. Mungan, Phys. Rev. E **53**, 6435 (1996).
[8] A. Kudrolli, M. Wolpert, and J. P. Gollub, Phys. Rev. Lett. **78**, 1383 (1997).
[9] A 256×256 pixel, 955 frame per second (fps) Dalsa-CA-D6 8 bit camera was used in a run-to- disk mode of 477 fps.
[10] Software analysis was done with programs written in the Interactive Data Language (IDL) available from Research Systems, Inc. in Boulder, Colorado.
[11] V. I. Arnold and A. Avez, *Ergodic Problems of Classical Mechanics* (Addison-Wesley, Reading, MA, 1989).